

Color-adjustable phosphors $\text{Sr}_4\text{La}(\text{PO}_4)_3\text{O}:\text{Ce}^{3+},\text{Tb}^{3+},\text{Mn}^{2+}$ impact on luminescence of white light-emitting diodes

My Hanh Nguyen Thi¹, Phan Xuan Le²

¹Faculty of Mechanical Engineering, Industrial University of Ho Chi Minh City, Ho Chi Minh City, Vietnam

²Faculty of Mechanical-Electrical and Computer Engineering, School of Engineering and Technology, Van Lang University, Ho Chi Minh City, Vietnam

Article Info

Article history:

Received Nov 28, 2021

Revised Jun 16, 2022

Accepted Jun 25, 2022

Keywords:

Color homogeneity

Luminous flux

Monte Carlo theory

$\text{Sr}_4\text{La}(\text{PO}_4)_3\text{O}$

WLEDs

ABSTRACT

We used the ceramic approach to synthesize a sequence of $\text{Sr}_4\text{La}(\text{PO}_4)_3\text{O}:\text{Ce}^{3+},\text{Tb}^{3+},\text{Mn}^{2+}$ within our study. Especially, the attributes of $\text{Sr}_4\text{La}(\text{PO}_4)_3\text{O}$ that were extensively investigate are luminous characteristics, thermal stablesness, and energy transferring between Ce^{3+} and Tb^{3+} as well as Mn^{2+} . Through power shift, sensitizer Ce^{3+} ions can considerably boost the fragile green radiation from Tb^{3+} and red radiation from Mn^{2+} . The color of the radiation can be changed by adjusting the $\text{Ce}^{3+}/\text{Tb}^{3+}$ and $\text{Ce}^{3+}/\text{Mn}^{2+}$ ion ratios. The $\text{Sr}_4\text{La}(\text{PO}_4)_3\text{O}:0.12\text{Ce}^{3+},0.3\text{Mn}^{2+}$ specimen produced white light having hue coordinates of (0.3326, 0.3298). According to this result, it shows that $\text{Sr}_4\text{La}(\text{PO}_4)_3\text{O}:\text{Ce}^{3+},\text{Tb}^{3+},\text{Mn}^{2+}$ might be used in white light-emitting diodes (WLEDs).

This is an open access article under the [CC BY-SA](https://creativecommons.org/licenses/by-sa/4.0/) license.



Corresponding Author:

Phan Xuan Le

Faculty of Mechanical-Electrical and Computer Engineering, School of Engineering and Technology

Van Lang University

Ho Chi Minh City, Vietnam

Email: le.px@vlu.edu.vn

1. INTRODUCTION

White light-emitting diodes (WLEDs) are commonly employed and have attracted numerous commercial attention as solid-state illuminations as they have extended lifespan, small power consumption, tiny size, and environmental friendliness [1], [2]. Creating a merger between one blue InGaN chip and yellow-color YAG:Ce would be now the most popular method to generate white illumination [3]. Without sufficient red illumination, such a type of white radiation has a small hue rendering indicator (CRI \approx 70-80) as well as a huge correlated hue temperature (CCT \approx 7500 K) [4], [5]. Many scientists have been studying red phosphors that are triggerable using blue lighting in recent years. The phosphor-transformed WLEDs could have poor correlated color temperature (CCT) and elevated colour rendering index (CRI) using these phosphors such as $\text{Na}_5\text{Ln}(\text{MoO}_4)_4:\text{Eu}^{3+}$ (Ln=La, Gd, Y) [6], $\text{CaS}:\text{Eu}^{2+}$ [7], $\text{CaAlSiN}_3:\text{Eu}^{2+}$ [8], and $\text{K}_2\text{SiF}_6:\text{Mn}^{4+}$ [9], [10]. Unfortunately, there are two primary issues. First problem is the poor blue radiation effectiveness owing to severe re-absorption between phosphors emitting green and red lighting. The second problem is high manufacturing costs. As a result, several investigations have concentrated on producing efficient, long-lasting, single-phase phosphors that emit white lighting with red, green, and blue (RGB) elements via the power shift between sensitizes and triggers [11], [12]. A typical technique for achieving white light is co-doping ions of Ce^{3+} , Tb^{3+} , or Mn^{2+} through power shift for one-stage phosphors [11]–[13]. Ce^{3+} exhibits conventional parity permitted $5d-4f$ electronic shifts because it possesses a $4f^15d^0$ ground state and a $4f^05d^1$ excited state. Since the host lattice strongly influences the distribution of Ce^{3+} energy degree.

Explained for the radiation from the 5d-4f transition occur over a wide wavelength range. The ions Tb^{3+} and Mn^{2+} have both been employed as green and red radiation elements in the past. Owing to the prohibited 4f-4f shift for Tb^{3+} as well as ${}^4T_1-{}^6A_1$ transitions for Mn^{2+} , the excitation bands of Tb^{3+} as well as Mn^{2+} ions between ultraviolet (UV) and the area that is possible to be seen, are very faint [14], [15]. A common way to increase the absorption of Tb^{3+} and Mn^{2+} in the UV region would be using an effective sensitizer, like Ce^{3+} , and transfer the forcefully absorbed stimulation power from 5d level of Ce^{3+} to level of ${}^5D_{3,4}$ Tb^{3+} or 4G level of Mn^{2+} 's [11], [16], [17]. Emission-tunable single-phase phosphors are achievable using this method, which also saves manufacturing costs, and increases color repeatability and luminescence efficiency [18], [19]. Because of the excellent physical and chemical steadiness of them, apatite has been considered as an effective host material for phosphors until now [20]–[24]. $Sr_4La(PO_4)_3O$ (SLPO) is isomorphic to the apatite complex. Furthermore, it also includes two cation locations, a nine-fold coordination 4f location having C_3 point symmetry, as well as a seven-fold coordination 6h location having C_s point symmetry [21]. From earlier research of ours, the SLPO: $Eu^{3+}/Tb^{3+}/Ce^{3+}$ phosphors have been examined [22]. Tb^{3+} or Mn^{2+} were injected into SLPO: Ce^{3+} in this study. While including power shift in the process to obtain a green radiation maximum of Tb^{3+} under 539 nm as well as a red radiation range for Mn^{2+} having the highest point under roughly 605 nm. We also extensively investigated their photoluminescence characteristics along with power shifts between Ce^{3+} and Tb^{3+} as well as Mn^{2+} . Through altering the dopant concentration for Tb^{3+} or Mn^{2+} , we can achieve adjustable discharge hues ranging between blue and green as well as warm white, implying a prospective application in UV-pumped WLEDs.

2. EXPERIMENTAL DETAILS

2.1. Creating phosphor substances

The traditional high-temperature solid-state process is our choice to make $Sr_4La_{1-x-y}(PO_4)_3O: xCe^{3+}, yTb^{3+}$, and $Sr_{4-z}La_{1-x}(PO_4)_3O: xCe^{3+}, zMn^{2+}$ phosphors with various compositions. Including these starting materials: $SrCO_3$ (99%), $(NH_4)_2HPO_4$ (99%), La_2O_3 (99.99%), Tb_4O_7 (99.99%), $MnCO_3$ (99%) along with CeO_2 (99.99%). The flux is 2wt% Li_2CO_3 (99%). In terms of combine and grind, an agate mortar was used to achieve the stoichiometric starting reagents. The combination was fired for the first time in the air for 3 hours at 600 °C, and ground again. Then, we calcined it in a decreasing environment (N₂:H₂=95:5) for 5 hours at 1200 °C. An ARL X'TRA powder X-ray diffractometer having Cu K α radiation ($\lambda=1.5406$ Å) running under 40 kilovolts along with the presence of 35 mA is to assist in measuring the phase purity. Diffuse reflection spectra (DRS) in the 200-700 nm range were acquired using a UV/visible spectrophotometer that utilizes $BaSO_4$ in the form of a reference. Next, we use a field emission scanning electron microscope for the task of analyzing the morphologies for the as-prepared specimens. With an Edinburgh FS5 fluorescence spectrophotometer amidst one xenon light working under 150 watts as the illumination source, we obtained the photoluminescence excitation (PLE) as well as photoluminescence (PL) spectra. We put the samples above a warming apparatus heatable between 25 and 200 °C accompanied by a 1 °C step. We use the FS5 spectrofluorometer system to measure the temperature. Then, we determine the samples' photoluminescent extrinsic quantum yields by a globe for the FS5 spectrophotometer. An Edinburgh FLS 920 Fluorescence Spectrophotometer was used to measure the fluorescence lifetime.

2.2. Preparation of phosphor materials

The most suitable linear fitting around the absorbing rim may be attained using n value of 2 between the plots of $[F(R)hv]^2$, $[F(R)h]$, $[F(R)h]^{2/3}$, $[F(R)h]^{1/2}$, and $[F(R)h]^{1/3}$ through the photon power hv . The plot of $[F(R)h]$ versus hv is shown in the inset of Figure 1. The SLPO optic bandgap (3.85 eV) can be calculated through extrapolating the linear fit to $[F(R)h] = 0$.

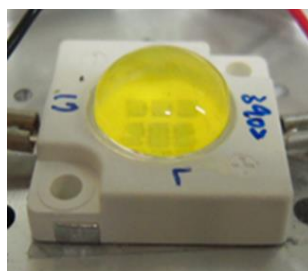


Figure 1. WLEDs photograph

The absorption spectra for SLPO were attained from the reflecting band of colors utilizing the Kubelka-Munk (K-M) function for the task of calculating the optic bandgap for the SLPO combination [25].

$$F(R) = \frac{(1-R)^2}{2R} = K/S \quad (1)$$

The reflection, absorption, and scattering coefficients are R, K, and S, respectively. The Tau relation [26] connects the bandgap E_g and linear absorbing factor of a substance:

$$ahv \propto (hv - E_g)^{n/2} \quad (2)$$

v indicates the photon power. n values of 1, 2, 3, 4, and 6 correspond to direct permitted shifts, non-metal substances, directly prohibited shifts, indirectly permitted shifts, as well as indirect prohibited shifts [26]. When the substance disperses in a fully diffuse manner, the absorbing factor K equals 2α . Because the dispersing factor S is a constant relative to the wavelength, equation (1) and (2) can be used to express as (3).

$$[F(R)hv]^2 \propto (hv - E_g)^n \quad (3)$$

The phosphor film in the MCW-LED device would be replicated using flat silicone sheets via the LightTools 9.0 application and the Monte Carlo approach. This simulation takes place through two distinct times: (1) It is critical to establish and create MCW-LED lamp configuration models and optical characteristics (2). The optical impacts of phosphor compounding are then properly controlled by the $\text{Sr}_4\text{La}(\text{PO}_4)_3\text{O}:\text{Ce}^{3+},\text{Tb}^{3+},\text{Mn}^{2+}$ concentration variety. We must establish several contrasts to determine the effect of $\text{YAG}:\text{Ce}^{3+}$ and $\text{Sr}_4\text{La}(\text{PO}_4)_3\text{O}:\text{Ce}^{3+},\text{Tb}^{3+},\text{Mn}^{2+}$ phosphor combination on the output of MCW-LED lamps. Dual-layer distant phosphorus, described as two types of compounds with mean CCTs of 3000 K, 4000 K, and 5000 K, is to be elucidated. Figure 1 depicts MCW-LED lamps with a protective-coating phosphor combination and an average CCT of 8500 K in detail. The simulation of MCW-LEDs without $\text{Sr}_4\text{La}(\text{PO}_4)_3\text{O}:\text{Ce}^{3+},\text{Tb}^{3+},\text{Mn}^{2+}$ is also recommended. The reflector's bottom lengthiness reaches 8 mm, pitch reaches 2.07 mm, and above exterior lengthiness reaches 9.85 mm. The protective-coating phosphor combination will be applied to nine chips having a 0.08-mm thickness. All LED chips would be connected to the reflector's gap by a square zone of 1.14-mm² as well as a pitch measured at 0.15 mm. The radiance flux for a chip would be 1.16 W, with a maximal wavelength of 453 nm.

3. RESULTS AND ANALYSIS

Figure 2 illustrates the reversal shift in the concentrations of $\text{Sr}_4\text{La}(\text{PO}_4)_3\text{O}:\text{Ce}^{3+},\text{Tb}^{3+},\text{Mn}^{2+}$ (Sr:Ce,Tb,Mn) as well as $\text{YAG}:\text{Ce}^{3+}$, under CCTs of 5700 K and 8000 K in Figure 2(a) and (b), respectively. Such an adjustment serves specific purposes: keeping mean CCTs the same, and affecting the absorptivity as well as dispersing in WLEDs with two phosphor layers. This, in turn, affects the hue standard as well as lighting ray performance in WLEDs. The color quality of WLEDs is thus determined by the Sr:Ce,Tb,Mn concentration chosen. When the Sr:Ce,Tb,Mn ratio increased (2%-20% Wt.), the $\text{YAG}:\text{Ce}^{3+}$ concentration was reduced for the task of sustaining the mean CCTs. It is also true for WLEDs with color heats ranging between 5700 K and 8000 K.

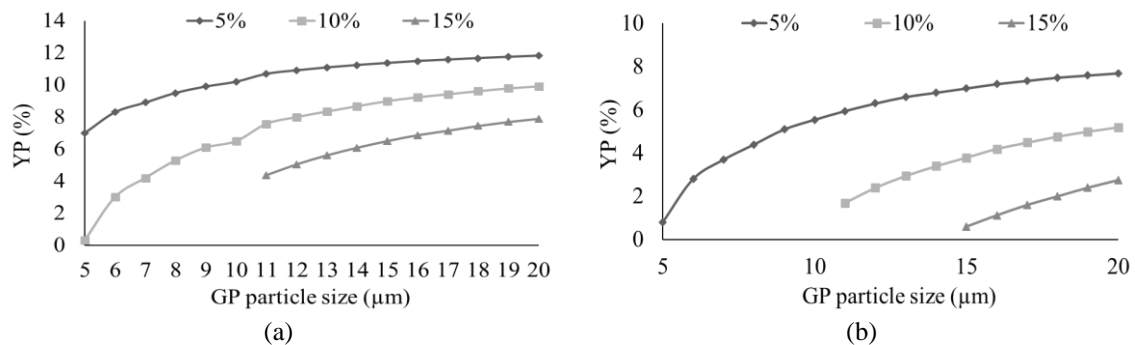


Figure 2. Altering phosphor concentration for the task of sustaining median CCT, (a) 5700 K and (b) 8000 K

Figure 3 depicts the influence of the Sr:Ce,Tb,Mn green phosphorus concentration on the transmitting band of colors in the WLED device under CCTs of 5700 K and 8000 K in Figure 3(a) and (b), respectively. We can pick a suitable option by considering the demands of the producers. WLED devices with good colour consistency will yield a minor lumen penalty. The amalgam of the spectrum zone will yield white illumination, a result demonstrated by Figure 3. The Figure demonstrates one spectrum measured at 5000 K. As can be seen easily, the strength trend increases with concentration Sr:Ce,Tb,Mn in two sections of the light spectrum: 420-480 nm as well as 500-640 nm. Such a rise for the luminous flux may be seen via the discharge spectrum with two lines. Additionally, the blue illumination dispersing within the WLED device increased. Consequently, the dispersing within the sheet of phosphor as well as WLED device will increase as well, and favoring colour uniformity. When Sr:Ce,Tb,Mn is presented, a remarkable result may occur. The colour consistency in the remote phosphor configuration with huge temperature would be challenging to control. Our research found that Sr:Ce,Tb,Mn, under small as well as huge colour temperatures (5600 K as well as 8500 K), can augment the colour standard in the WLED device.

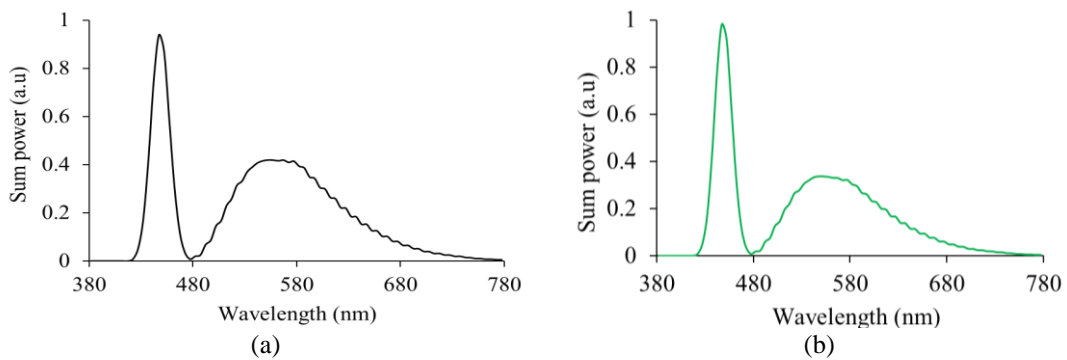


Figure 3. The radiation spectra in the WLED device along with Sr:Ce,Tb,Mn concentration: (a) 5700 K and (b) 8000 K

The efficiency for the lumen of the dual-sheet phosphor layout was further demonstrated in the paper. As the Sr:Ce,Tb,Mn content increased (2%-20% wt.), the lumen emitted increased dramatically, a result demonstrated by Figure 4, under CCTs of 5700 K and 8000 K in Figure 4(a) and (b), respectively. (Figure 5), the colour aberration suffered from an enormous penalty alongside the Sr:Ce,Tb,Mn concentration, under CCTs of 5700 K and 8000 K in Figure 5(a) and (b), respectively. The absorptivity from the red phosphor sheet may be the cause of such an event. When the Sr:Ce,Tb,Mn phosphor swallowed the blue illumination from the LED chip, the blue illumination is converted into the green illumination. The Sr:Ce,Tb,Mn particles still embodied the yellow light, besides the blue illumination generated by the chip. On the other hand, with the absorptivity of the substance, the blue light absorption from the LED chip appears to be more potent, surpassing said absorptivities. With Sr:Ce,Tb,Mn, the green illumination content for the WLED device rises, improving the colour uniformity index. Colour uniformity is one of the most necessary elements among current WLED light parameters. The higher the colour uniformity index, the pricier the WLED. But Sr:Ce,Tb,Mn proves to be inexpensive and can thus be used in a variety of applications.

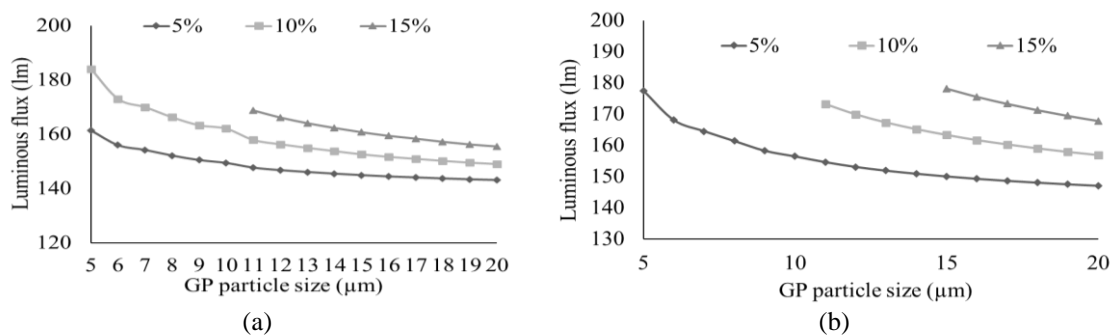


Figure 4. The illuminating beam in the WLED device along with Sr:Ce,Tb,Mn concentration, (a) 5700 K and (b) 8000 K

Colour consistency would be the sole factor for examining WLED colour output. Colour quality is claimed to be badly affected by colour homogeneity index. As a result, recent studies have developed a colour rendering index (CRI) and a colour quality scale (CQS). As CRI is illuminated, it displays the true colour of an object. Too much green illumination between the three principal colours: blue, yellow, as well as green, causes the colour imbalance. This has an effect on the colour quality of WLEDs, causing inferior colour consistency. A minor CRI penalty in the existence of the remote phosphor Sr:Ce,Tb,Mn layer is demonstrated by Figure 6, under CCTs of 5700 K and 8000 K in Figure 6(a) and (b), respectively.

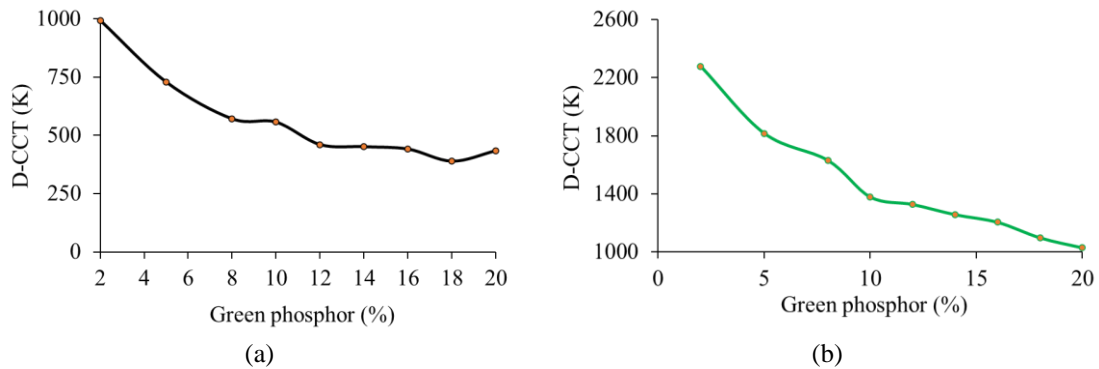


Figure 5. The colour deviation in the WLED device along with Sr:Ce,Tb,Mn concentration (a) 5700 K and (b) 8000K

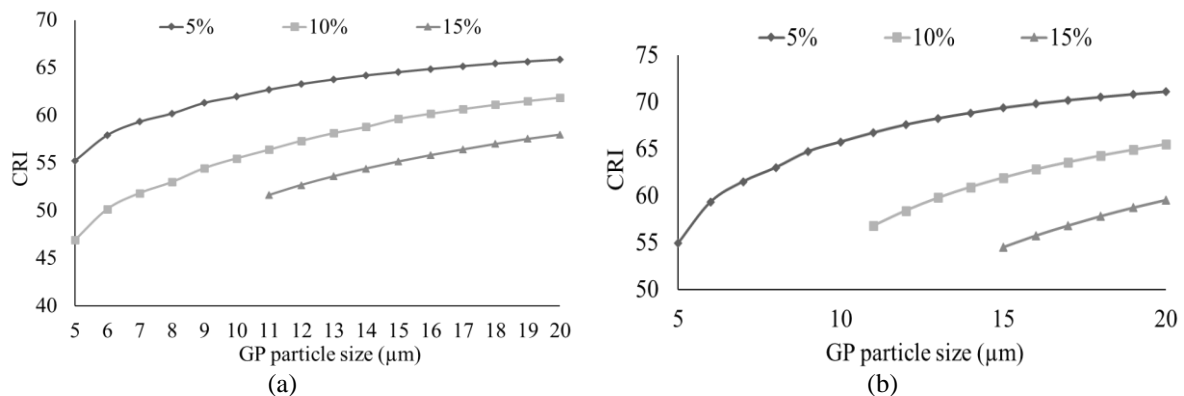


Figure 6. The colour rendering indicator in the WLED device along with Sr:Ce,Tb,Mn concentration, (a) 5700 K and (b) 8000K

However, such a penalty would be acceptable. The CQS would be of greater importance and is harder to attain than CRI. CQS is an index with three facets, consisting of CRI, beholder's taste, along with colour coordinate. For these essential facets, CQS is almost a genuine overall assessment of colour quality. An augmentation for CQS caused by the Sr:Ce,Tb,Mn layer is demonstrated by Figure 7, under CCTs of 5700 K and 8000 K in Figure 7(a) and (b), respectively. When the Sr:Ce,Tb,Mn concentration rise, CQS is barely altered as the Sr:Ce,Tb,Mn concentration goes below 10% wt., CRI, along with CQS, is substantially diminished when Sr:Ce,Tb,Mn contents rise above 10% wt., a result of significant waste of colour if green becomes dominant. Hence, if we utilize Sr:Ce,Tb,Mn, proper concentration selection is critical.

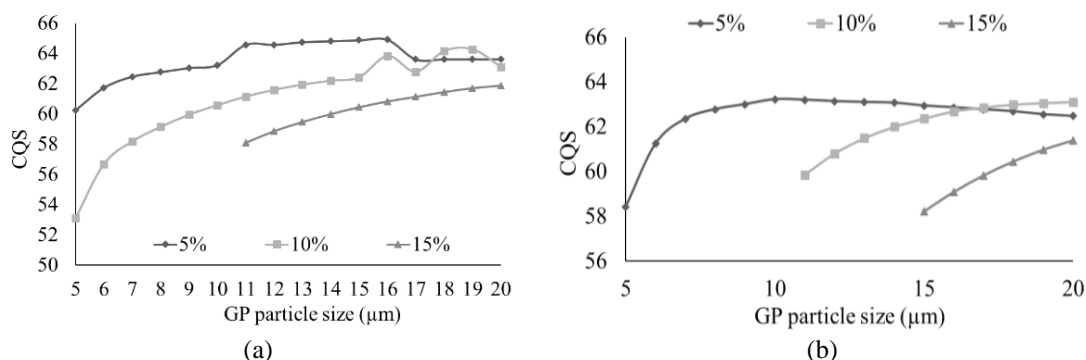


Figure 7. The colour standard scale of WLEDs as a function of Sr:Ce,Tb,Mn concentration: (a) 5700 K and (b) 8000K

4. CONCLUSION

The typical solid-state procedure was used to make a series of SLPO:0.12Ce³⁺,yTb³⁺ as well as SLPO:0.12Ce³⁺, zMn²⁺. We also focus on the power shifts between Ce³⁺ and Tb³⁺ as well as between Ce³⁺ and Mn²⁺. Dipole-dipole interaction dominated the processes of the two-power shift. The concentration of Tb³⁺ or Mn²⁺ ions can be adjusted to accomplish several emission hues ranging between green-blue and green or white. With the stimulation of 310 nm UV-light, it is possible to acquire white illumination discharge having a CIE of (0.3326, 0.3298) in the SLPO: 0.12Ce³⁺, 0.3Mn²⁺ phosphor. Because of advancements in semiconductor, chips used in synthesizing phosphors in LEDs may now be made with a variety of emitting wavelengths, indicating that the SLPO: Ce³⁺/Tb³⁺/Mn²⁺ would be a great one-stage phosphor to be used in WLED.

ACKNOWLEDGEMENTS

This study was financially supported by Van Lang University, Vietnam.




REFERENCES

- [1] S.-R. Chung, C.-B. Siao, and K.-W. Wang, "Full color display fabricated by CdSe bi-color quantum dots-based white light-emitting diodes," *Optical Materials Express*, vol. 8, no. 9, p. 2677, Sep. 2018, doi: 10.1364/ome.8.002677.
- [2] J. Zhang, L. Zhao, X. Bian, and G. Chen, "Ce³⁺/Mn²⁺-activated Ca₇(PO₄)₂(SiO₄)₂: efficient luminescent materials for multifunctional applications," *Optics Express*, vol. 26, no. 18, p. A904, Sep. 2018, doi: 10.1364/oe.26.00a904.
- [3] T. Kozacki, M. Chlipala, and H.-G. Choo, "Fourier rainbow holography," *Optics Express*, vol. 26, no. 19, p. 25086, Sep. 2018, doi: 10.1364/oe.26.025086.
- [4] C. Han *et al.*, "Effect of surface recombination in high performance white-light CH₃NH₃PbI₃ single crystal photodetectors," *Optics Express*, vol. 26, no. 20, p. 26307, Oct. 2018, doi: 10.1364/oe.26.026307.
- [5] O. H. Kwon, J. S. Kim, J. W. Jang, and Y. S. Cho, "Simple prismatic patterning approach for nearly room-temperature processed planar remote phosphor layers for enhanced white luminescence efficiency," *Optical Materials Express*, vol. 8, no. 10, p. 3230, Oct. 2018, doi: 10.1364/ome.8.003230.
- [6] X. Leng *et al.*, "Feasibility of co-registered ultrasound and acoustic-resolution photoacoustic imaging of human colorectal cancer," *Biomedical Optics Express*, vol. 9, no. 11, p. 5159, Nov. 2018, doi: 10.1364/boe.9.005159.
- [7] Y. Tang, Z. Li, G. Liang, Z. Li, J. Li, and B. Yu, "Enhancement of luminous efficacy for LED lamps by introducing polyacrylonitrile electrospinning nanofiber film," *Optics Express*, vol. 26, no. 21, p. 27716, Oct. 2018, doi: 10.1364/oe.26.027716.
- [8] X. Bao, X. Gu, and W. Zhang, "User-centric quality of experience optimized resource allocation algorithm in VLC network with multi-color LED," *Optics Express*, vol. 26, no. 21, p. 27826, Oct. 2018, doi: 10.1364/oe.26.027826.
- [9] B. Li *et al.*, "High-efficiency cubic-phased blue-emitting Ba₃Lu₂B₆O₁₅:Ce³⁺ phosphors for ultraviolet-excited white-light-emitting diodes," *Optics Letters*, vol. 43, no. 20, p. 5138, Oct. 2018, doi: 10.1364/ol.43.005138.
- [10] V. Bahrami-Yekta and T. Tiedje, "Limiting efficiency of indoor silicon photovoltaic devices," *Optics Express*, vol. 26, no. 22, p. 28238, Oct. 2018, doi: 10.1364/oe.26.028238.
- [11] X. Li, B. Hussain, L. Wang, J. Jiang, and C. Patrick Yue, "Design of a 2.2-mW 24-Mb/s CMOS VLC Receiver SoC with Ambient Light Rejection and Post-Equalization for Li-Fi Applications," *Journal of Lightwave Technology*, vol. 36, no. 12, pp. 2366–2375, Jun. 2018, doi: 10.1109/JLT.2018.2813302.
- [12] X. Ding *et al.*, "Improving the optical performance of multi-chip LEDs by using patterned phosphor configurations," *Optics Express*, vol. 26, no. 6, p. A283, Mar. 2018, doi: 10.1364/oe.26.00a283.
- [13] H.-Y. Yu *et al.*, "Solar spectrum matching with white OLED and monochromatic LEDs," *Applied Optics*, vol. 57, no. 10, p. 2659, Apr. 2018, doi: 10.1364/ao.57.002659.
- [14] Q. Guo *et al.*, "Characterization of YAG:Ce phosphor dosimeter by the co-precipitation method for radiotherapy," *Applied Optics*, vol. 60, no. 11, p. 3044, Apr. 2021, doi: 10.1364/ao.419800.
- [15] H. Yuce, T. Guner, S. Balci, and M. M. Demir, "Phosphor-based white LED by various glassy particles: control over luminous efficiency," *Optics Letters*, vol. 44, no. 3, p. 479, Feb. 2019, doi: 10.1364/ol.44.000479.




- [16] L. Yang, Q. Zhang, F. Li, A. Xie, L. Mao, and J. Ma, "Thermally stable lead-free phosphor in glass enhancement performance of light emitting diodes application," *Applied Optics*, vol. 58, no. 15, p. 4099, May 2019, doi: 10.1364/ao.58.004099.
- [17] A. M. Nahavandi, M. Safi, P. Ojaghi, and J. Y. Hardeberg, "LED primary selection algorithms for simulation of CIE standard illuminants," *Optics Express*, vol. 28, no. 23, p. 34390, Nov. 2020, doi: 10.1364/oe.408754.
- [18] V.-C. Su and C.-C. Gao, "Remote GaN metalens applied to white light-emitting diodes," *Optics Express*, vol. 28, no. 26, p. 38883, Dec. 2020, doi: 10.1364/oe.411525.
- [19] F. B. Chen, K. L. Chi, W. Y. Yen, J. K. Sheu, M. L. Lee, and J. W. Shi, "Investigation on Modulation Speed of Photon-Recycling White Light-Emitting Diodes with Vertical-Conduction Structure," *Journal of Lightwave Technology*, vol. 37, no. 4, pp. 1225–1230, Feb. 2019, doi: 10.1109/JLT.2018.2890331.
- [20] S. Xu *et al.*, "Exploration of yellow-emitting phosphors for white LEDs from natural resources," *Applied Optics*, vol. 60, no. 16, p. 4716, Jun. 2021, doi: 10.1364/ao.424108.
- [21] S. Keshri *et al.*, "Stacked volume holographic gratings for extending the operational wavelength range in LED and solar applications," *Applied Optics*, vol. 59, no. 8, p. 2569, Mar. 2020, doi: 10.1364/ao.383577.
- [22] X. Xi *et al.*, "Chip-level Ce:GdYAG ceramic phosphors with excellent chromaticity parameters for high-brightness white LED device," *Optics Express*, vol. 29, no. 8, p. 11938, Apr. 2021, doi: 10.1364/oe.416486.
- [23] H. S. El-Ghoroury, Y. Nakajima, M. Yeh, E. Liang, C.-L. Chuang, and J. C. Chen, "Color temperature tunable white light based on monolithic color-tunable light emitting diodes," *Optics Express*, vol. 28, no. 2, p. 1206, Jan. 2020, doi: 10.1364/oe.375320.
- [24] P. Zhu, H. Zhu, G. C. Adhikari, and S. Thapa, "Spectral optimization of white light from hybrid metal halide perovskites," *OSA Continuum*, vol. 2, no. 6, p. 1880, Jun. 2019, doi: 10.1364/osac.2.001880.
- [25] W.-Y. Chang, Y. Kuo, Y.-W. Kiang, and C. C. Yang, "Simulation study on light color conversion enhancement through surface plasmon coupling," *Optics Express*, vol. 27, no. 12, p. A629, Jun. 2019, doi: 10.1364/oe.27.00a629.
- [26] K. Orzechowski, M. M. Sala-Tefelska, M. W. Sierakowski, T. R. Woliński, O. Strzeczysz, and P. Kula, "Optical properties of cubic blue phase liquid crystal in photonic microstructures," *Optics Express*, vol. 27, no. 10, p. 14270, May 2019, doi: 10.1364/oe.27.014270.

BIOGRAPHIES OF AUTHORS



My Hanh Nguyen Thi    received a Bachelor of Physics from An Giang University, Viet Nam, Master of Theoretical Physics And Mathematical Physics, Hanoi National University of Education, Viet Nam. Currently, she is a lecturer at the Faculty of Mechanical Engineering, Industrial University of Ho Chi Minh City, Viet Nam. Her research interests are Theoretical Physics and Mathematical Physics. She can be contacted at email: nguyenthimyanh@iuh.edu.vn.



Phan Xuan Le    received a Ph.D. in Mechanical and Electrical Engineering from Kunming University of Science and Technology, Kunming City, Yunnan Province, China. Currently, he is a lecturer at the Faculty of Engineering, Van Lang University, Ho Chi Minh City, Viet Nam. His research interests are optoelectronics (LED), power transmission and automation equipment. He can be contacted at email: le.px@vlu.edu.vn.